Open access • Journal Article • DOI:10.1029/94JA02572

Electron temperature effects in the linear proton mirror instability — Source link

F.G.E Pantellini, Steven J. Schwartz

Institutions: Queen Mary University of London

Published on: 01 Mar 1995 - Journal of Geophysical Research (John Wiley & Sons, Ltd)

Topics: Electric field, Proton, Linear polarization, Electron and Magnetic field

Electron temperature effects in the linear proton mirror instability

Filippo Pantellini, S. J. Schwartz

Pantellini, F. G. E., and Schwartz, S. J. (1995), Electron temperature effects in the linear proton mirror instability, *J. Geophys. Res.*, 100(A3), 3539– 3549, doi:10.1029/94JA02572.

JOURNAL OF GEOPHYSICAL RESEARCH, VOL. 100, NO. A3, PAGES 3539–3549, MARCH 1, 1995

Electron temperature effects in the linear proton mirror instability

F.G.E. Pantellini[1] and S.J. Schwartz

Astronomy Unit, Queen Mary and Westfield College, London, England, United Kingdom

Abstract. It is shown that when the electron temperature T_e is of the same order of the proton temperature parallel to the background magnetic field, the growth rate of the proton mirror mode in the long-wavelength limit is reduced by the presence of a longitudinal electric field. The field is due to the electron pressure gradient which builds up when $T_e \neq 0$, because the electrons are dragged by nonresonant protons which are mirror accelerated from regions of high into regions of low parallel magnetic field flux. In return, the longitudinal electric field causes the density of nonresonant protons with a perpendicular velocity smaller than a strongly T_e-dependent critical velocity $v_{\perp,\mathrm{crit}}$ to increase (decrease) at maxima (minima) of the parallel magnetic field flux. These nonresonant protons thus behave differently from the "circulating" protons described by Southwood and Kivelson (1993) in the cold electron limit. Although the instability threshold is only weakly affected by changes in T_e, quantities like the growth rate, the compressibility, the polarization, and the angle between wave vector and magnetic field for the most unstable mode, as well as the structure of the perturbed proton distribution itself, are strongly modified by variations in the electron temperature. The predictions of the model are shown to agree well with numerical solutions of the full Vlasov dispersion relation, indicating that most long-wavelength aspects of the proton mirror instability are included in the model.

1. Introduction

The proton mirror instability is a nonpropagating, slowly growing (less than proton cyclotron frequency) long-wavelength (greater than proton Larmor radius) instability driven by a pressure anisotropy $p_\perp/p_\parallel > 1$ where the perpendicular and parallel subscripts refer to the direction of the zeroth order magnetic field. The minimum anisotropy required to destabilize the mode generally depends on other plasma parameters. For example, in a homogeneous and spatially uniform magnetized bi-Maxwellian proton plasma with cold electrons (number density N_0) the instability threshold depends on the ratio $\beta_\perp$ between the perpendicular proton pressure $p_\perp = N_0 T_\perp$ (temperatures are assumed to be multiplied by the Boltzmann constant throughout the paper) and the magnetic field pressure $B_0^2/8\pi$ and is given by $T_\perp/T_\parallel = 1 + 1/\beta_\perp$ [e.g., *Hasegawa*, 1969].

Although the mirror instability has been known for some time [e.g., *Chandrasekhar*, 1958], it has been revisited by a number of authors. As a first step, *Rose* [1965] pointed out how critically the instability threshold depends on the details of the proton distribution at small parallel velocities. Later, *Barnes* [1966] and *Tajiri* [1967], for the case of hot electrons, and *Hasegawa* [1969], for the case of a nonuniform medium, numerically solved the kinetic dispersion relation in the low-frequency and long-wavelength limit. The kinetic treatments revealed that the dispersion relations obtained from fluid treatments are wrong in the prediction that the mirror mode is oscillating when the instability threshold is not exceeded. Furthermore, the growth rates deduced from fluid and kinetic theories differ by a nonnegligible numerical factor.

Until the first observations in the Earth's magnetosheath by *Kaufmann et al.* [1970] the major interest in the mirror instability was related to the problem of plasma confinement by a theta pinch in fusion experiments (see, for example, the collection of reprints published by *Jeffrey and Taniuti* [1966]). Since then, an increasingly large number of observations have confirmed the existence of the mirror instability in virtually all of the explored space plasmas where a proton temperature anisotropy can be generated by some mechanism. Besides the identification in the Earth's magnetosheath, e.g., well downstream from the quasi-perpendicular portion of the Earth bow shock [*Hubert et al.*, 1989], mirror waves have been observed at comets

[1]Now at Observatoire de Paris-Meudon, Département de Recherche Spatiale, Meudon, France.

Paper number 94JA02572.
0148-0227/95/94JA-02572$05.00

[*Russell et al.*, 1987] and in interplanetary space [*Tsurutani et al.*, 1992]. More recently, *Lacombe et al.* [1992] have reported the existence of mirror waves even in the overshoot of the quasi-perpendicular Earth bow shock, suggesting that mirror waves take part, at least in some cases, in the energy dissipation within the shock itself. Moreover, *Anderson and Fuselier* [1993] have shown that in the Earth's magnetosheath, mirror waves tend to occur when the proton temperature anisotropy is small (i.e., $T_\perp/T_\parallel \approx 1.5$) and the proton pressure is high (i.e. $\beta \gtrsim 5$).

Stimulated by the observations and favored by the rapidly increasing capabilities of modern computers, numerical simulations of the instability started to become fashionable during the last decade or so. Thus the one-dimensional simulations of *Price et al.* [1986] showed that the instability can be excited far downstream of supercritical, quasi-perpendicular shocks as a result of the proton temperature anisotropy generated in the shock ramp. *McKean et al.* [1993] investigated the distribution functions from hybrid simulations and found that in the case of slowly growing instability, the results do qualitatively agree with linear theory [*Southwood and Kivelson*, 1993]. Discrepancies are likely to be due to nonlinear effects [cf. *Pantellini et al.*, 1995]. *McKean et al.* [1993] also suggested that wave-particle energy exchanges in the linear instability tend to be most effective along magnetic slopes rather than at magnetic peaks or troughs.

By the end of the 1980s it became clear that another instability which develops under similar conditions, namely the Alfvén Ion Cyclotron (AIC) instability [e.g., *Davidson and Ogden*, 1975], usually has a faster linear growth rate than the mirror instability in a pure proton-electron plasma [*Lacombe et al.*, 1992; *Gary*, 1992], making it difficult to understand why the latter is observed at all. The predominance of the AIC instability over the mirror instability has been confirmed in one- and two-dimensional hybrid simulations [e.g., *McKean et al.*, 1992; *Winske and Quest*, 1988]. At least three possible explanations have been suggested for the fact that mirror waves are nevertheless observed in space plasmas. The first is that the alpha particles in the solar wind, which are usually neglected in numerical simulations, significantly reduce the growth of the AIC but not of the mirror instability [*Price et al.*, 1986; *Gary*, 1992]. The second is that at sufficiently high $\beta_\parallel$ and small temperature anisotropies and given the presence of the alpha particles, the mirror instability grows more rapidly than the AIC instability. Mirror waves have been observed under these conditions by *Anderson and Fuselier* [1993] and *Anderson et al.* [1994]. The third [*Southwood and Kivelson*, 1993] is that from the nonpropagating nature of the unstable mirror mode it follows that its linear development crucially depends on the spatial structure of the field. Such a spatial structure may exist in the plasma prior to the the development of the instability, namely at shocks. As a result, the AIC wave may not be able to grow in the structured field due to the fact that the proton cyclotron resonance condition (the base of the AIC instability) continually changes as the wave moves through the plasma, causing the efficiency of the resonance to be reduced. However, this mechanism has not yet been demonstrated to be efficient in numerical simulations.

The physical mechanism of the proton mirror instability has been investigated only very recently in the limit of cold electrons and small growth rates by *Southwood and Kivelson* [1993]. They pointed out that the growth of the instability crucially depends on the distribution of the Landau resonant protons ($v_\parallel \approx 0$) (see also *Rose* [1965]). This is the fundamental reason for the fluid models to fail in describing some of the main features of the mode such as the fact that it is damped, and not oscillating, below the stability threshold. Although cold electrons do allow for any longitudinal electric field to be short-circuited which, in turn, results in the plasma dispersion relation being much simpler [e.g., *Hasegawa*, 1969], it is clear that in the free solar wind (where the electrons are typically hotter than the protons) and even in the Earth's magnetosheath, the cold electron approximation won't apply in general. We show that besides a slight change to the instability threshold, taking into account the presence of hot electrons strongly modifies some of the characteristics of the proton mirror mode such as the growth rate, the wave's polarization, the compressibility, and even the perturbed proton distribution function. These effects are shown to be ultimately related to the longitudinal electric field which is generated by an electron pressure gradient through the wave. The latter arises because the electrons are dragged away from the regions of high into regions of low parallel magnetic field flux by the protons for which the mirror force dominates.

2. The Physical Model

We start from a spatially homogeneous electron-proton plasma permeated by a magnetic field $\mathbf{B}_0$ pointing in the z direction of a right-handed Cartesian system (x, y, z). The equilibrium electron distribution f_e is Maxwellian with an isotropic and nonzero temperature T_e, while the equilibrium proton distribution f_p is taken to be bi-Maxwellian with perpendicular and parallel temperatures $T_\perp$ and $T_\parallel$ (we use a subscript e for electron quantities for clarity but usually omit a subscript p for the proton quantities).

2.1. The Perturbed Proton and Electron Distribution Functions

Following *Southwood and Kivelson* [1993], we derive an expression for the linear response of the proton and electron distributions in a slowly growing wave (the long-wavelength limit). Accordingly, a change δB in the magnetic field strength produces a change in the

energy δW of a particle following the adiabatic expression [*Northrop*, 1963]

$$\frac{d}{dt}\delta W = \mu\frac{\partial}{\partial t}\delta B_\parallel$$

where $\mu = mv_\perp^2/(2B)$ is the magnetic moment of the particle. If in addition, a longitudinal electric field $\delta E_\parallel$ is present, then the total rate of change in the particle's energy δW contains the work done by this field, namely,

$$\frac{d}{dt}\delta W = \mu\frac{\partial}{\partial t}\delta B_\parallel + qv_\parallel\delta E_\parallel. \tag{1}$$

Noting that $\delta W_\perp = \mu\delta B_\parallel$ and $\delta W_\parallel = \delta W - \mu\delta B_\parallel$, one finds that the rate of change in the particle's perpendicular and parallel energy is given by

$$\frac{d}{dt}\delta W_\perp = \mu\frac{d}{dt}\delta B_\parallel \tag{2a}$$

$$\frac{d}{dt}\delta W_\parallel = \frac{d}{dt}\delta W - \mu\frac{d}{dt}\delta B_\parallel. \tag{2b}$$

Liouville's theorem states that phase space density is constant along particle trajectories. Writing the distribution function $f = f(t, \mathbf{x}, W_\perp, W_\parallel)$ as the sum of a spatially uniform equilibrium distribution $f_0 = f(W_\perp, W_\parallel)$ and a small perturbation $\delta f = \delta f(t, \mathbf{x}, W_\perp, W_\parallel)$, one obtains the linearized version of Liouville's theorem in the form

$$\frac{\partial}{\partial t}\delta f + \mathbf{v}\cdot\frac{\partial}{\partial \mathbf{x}}\delta f + \frac{d}{dt}\delta W_\perp\frac{\partial}{\partial W_\perp}\delta f + \frac{d}{dt}\delta W_\parallel\frac{\partial}{\partial W_\parallel}\delta f = 0.$$

Using $\partial/\partial t + \mathbf{v}\cdot\partial/\partial\mathbf{x} = d/dt$, we can rewrite this in the more compact form

$$\frac{d}{dt}\delta f = -\frac{d}{dt}\delta W_\perp\frac{\partial}{\partial W_\perp}\delta f - \frac{d}{dt}\delta W_\parallel\frac{\partial}{\partial W_\parallel}\delta f \tag{3}$$

Assuming perturbations $\propto \exp[i(k_\perp x + k_\parallel z) + \gamma t]$, one finds that the change of an initially bi-Maxwellian proton distribution is given by

$$\delta f_p = \left[\frac{\mu_p\delta B_\parallel}{T_\perp}\left(1 - \frac{T_\perp}{T_\parallel}\right)\right] f_p + \left[\frac{\gamma}{\gamma + ik_\parallel v_\parallel}\left(\mu_p\delta B_\parallel - \frac{e\delta E_\parallel}{ik_\parallel}\right) + \frac{e\delta E_\parallel}{ik_\parallel}\right]\frac{f_p}{T_\parallel} \tag{4}$$

while that of an initially Maxwellian electron distribution reads

$$\delta f_e = \left[\frac{\gamma}{\gamma + ik_\parallel v_\parallel}\left(\mu_e\delta B_\parallel + \frac{e\delta E_\parallel}{ik_\parallel}\right) - \frac{e\delta E_\parallel}{ik_\parallel}\right]\frac{f_e}{T_e}. \tag{5}$$

In order to compare the different terms in the expressions for the perturbed distribution functions, $\delta E_\parallel$ has to be determined as a function of $\delta B_\parallel$. This can be done by solving the Poisson equation which, in the case of a slowly growing wave (i.e., $\gamma \to 0$), simply reduces to a quasi-neutrality condition

$$\frac{\delta N_p}{N_0} - \frac{\delta N_e}{N_0} = 0 \tag{6}$$

where δN_p and δN_e can be obtained by taking the first moments of δf_p and δf_e respectively. Neglecting terms proportional to $\gamma/(\gamma + ik_\parallel v_\parallel)$, which is justified by the fact that their contribution to the density perturbations is small as $\gamma \to 0$ or more precisely as long as $|\delta N_P/N_0| \gg \sqrt{\pi}\gamma/(k_\parallel v_{T\parallel})$ (see (25)), one obtains the linear response for the density perturbation of the protons

$$\frac{\delta N_p}{N_0} = \frac{\delta B_\parallel}{B_0}\left(1 - \frac{T_\perp}{T_\parallel}\right) + \frac{e\delta E_\parallel}{ik_\parallel T_\parallel} \tag{7}$$

and similarly for the electrons

$$\frac{\delta N_e}{N_0} = -\frac{e\delta E_\parallel}{ik_\parallel T_e}. \tag{8}$$

Equation (8) is nothing else but the usual fluid equation $\nabla_\parallel\delta p_e = -eN_0\delta E_\parallel$ for isothermal electrons. The desired expression for $\delta E_\parallel$ is finally found by using the quasi-neutrality condition (6) which yields

$$\delta E_\parallel = \frac{\delta B_\parallel}{B_0}\left(\frac{T_\perp - T_\parallel}{T_e + T_\parallel}\right)\frac{ik_\parallel}{e}T_e. \tag{9}$$

The parallel electric field $\delta E_\parallel$ can now be eliminated from (4) and (5), and the following expressions for the perturbations of the distributions are obtained

$$\frac{\delta f_p}{f_p} = \left\{\frac{v_\perp^2}{v_{T\parallel}^2}\left(\frac{T_\parallel}{T_\perp} - 1\right) + \frac{\gamma}{(\gamma + ik_\parallel v_\parallel)}\left[\frac{v_\perp^2}{v_{T\parallel}^2} - \left(\frac{T_\perp}{T_\parallel} - 1\right)\frac{T_e}{T_e + T_\parallel}\right] + \left(\frac{T_\perp}{T_\parallel} - 1\right)\frac{T_e}{T_e + T_\parallel}\right\}\frac{\delta B_\parallel}{B_0} \tag{10}$$

$$\frac{\delta f_e}{f_e} = \left\{\frac{\gamma}{(\gamma + ik_\parallel v_\parallel)}\left[\frac{v_\perp^2}{v_e^2} + \frac{T_\perp - T_\parallel}{T_e + T_\parallel}\right] - \left(\frac{T_\perp - T_\parallel}{T_e + T_\parallel}\right)\right\}\frac{\delta B_\parallel}{B_0} \tag{11}$$

where the notations $v_{T\parallel} \equiv (2T_\parallel/m_p)^{1/2}$ and $v_e \equiv (2T_e/m_e)^{1/2}$ have been introduced.

For nonzero values of T_e the last term on the right-hand side of (10) is nonzero and of opposite sign compared to the first term in the same expression. If one ignores, for the moment, the presence of the resonant

protons associated with the second term, which are limited to the small region in velocity space $|v_\parallel| < \gamma/k_\parallel$, it appears that δf_p changes sign as $v_\perp$ exceeds some critical velocity $v_{\perp,\mathrm{crit}}$. This critical velocity can thus be determined by equating the magnitudes of the first and the last term on the right-hand side of (10) to give

$$v_{\perp,\mathrm{crit}} = v_{T\perp}\left(\frac{T_e}{T_e + T_\parallel}\right)^{1/2} \tag{12}$$

with $v_{T\perp} \equiv (2T_\perp/m_p)^{1/2}$ being the perpendicular thermal velocity of the protons. Protons with $v_\perp > v_{\perp,\mathrm{crit}}$ are the circulating protons which, owing to the action of the mirror force, are responsible for the characteristic anticorrelation between $\delta B_\parallel$ and δN_p [*Southwood and Kivelson*, 1993]. Protons with $v_\perp < v_{\perp,\mathrm{crit}}$, on the other hand, act in the opposite way in that they tend to accumulate in regions of high parallel magnetic field flux. A schematic picture of the forces acting on a nonresonant proton in a mirror wave is shown in Figure 1, which illustrates the spatial variation of the longitudinal electric and magnetic field fluctuations, as well as the density fluctuations of the nonresonant particles through one wavelength, and shows that the electrostatic force and the mirror force on a proton always act against each other. However, as it will be shown later (section 2.4), the combined effect of both forces on the nonresonant protons (i.e., protons with $|v_\parallel| > \gamma/k_\parallel$) is such that the anticorrelation between δN and $\delta B_\parallel$ is always preserved even for large electron temperatures.

To understand the reason for the response δf_p of the proton distribution to the longitudinal electric field being of opposite sign with respect to the response to the mirror field, we consider the motion of protons, which are initially (i.e. at $t = -\infty$) on a contour of constant phase space density (Figure 2, stippled thick contour). We then use Liouville's theorem, which states that the phase space density is constant along a particle's trajectory, to determine the deformation of the contour in the field of the growing wave. In Figure 2 we have chosen the end position of the protons (at an arbitrary time) to coincide with the position of a magnetic field maximum. It is obvious that the trajectories of particles reaching a magnetic field minimum are just the same but with a reversed sign.

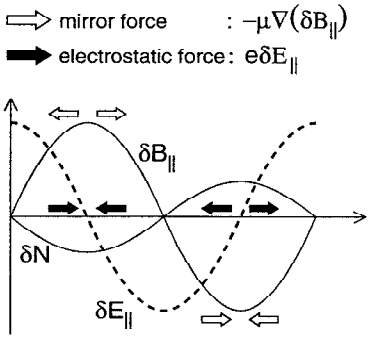

Figure 1. Spatial dependence of δN, $\delta B_\parallel$ (solid curves) and $\delta E_\parallel$ (dashed curve) through one wavelength. All curves are in arbitrary units. The arrows denote the mirror and the electrostatic force acting on a proton, at a minimum, as well as a maximum, of the parallel magnetic field strength. As shown the two forces act against each other, and since the mirror force is proportional to $v_\perp^2$, the electrostatic force can dominate the motion of protons with a small $v_\perp$.

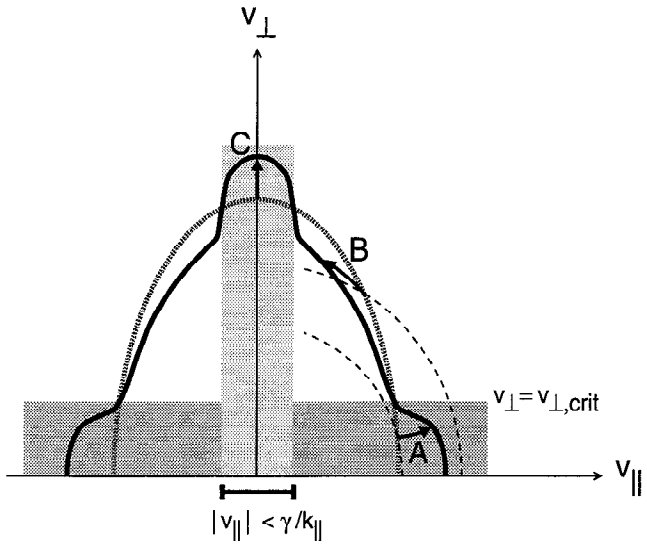

Figure 2. Sketch of the distortion of a proton phase space contour (thick solid line) in the linear mirror instability at a maximum of the magnetic field flux. The labeled arrows indicate the path, starting from the initial equilibrium distribution (thick stippled line), of three distinct types of protons (labeled A, B and C) which exist in the case of a nonzero T_e.

Let's first consider a nonresonant proton with $v_\perp = 0$, i.e., a proton which is not sensitive to the mirror force. On its way to a region of high magnetic field flux such a proton sees its parallel velocity being increased, owing to the fact that the electrostatic potential has a minimum there. Since the particle's perpendicular velocity is not changing, its trajectory in velocity space must go along a path of increasing $|v_\parallel|$. For protons with a nonzero initial perpendicular velocity, $v_\perp$ increases on its way toward a maximum of the magnetic field flux owing to the conservation of the magnetic moment. However, for protons with a small $v_\perp \ll v_{\perp,\mathrm{crit}}$ the mirror force is still insignificant and the behavior is similar to that of particles with $v_\perp = 0$ (Figure 2, type A trajectories). On the other hand, protons with $v_\perp \gg v_{\perp,\mathrm{crit}}$ (Figure 2, type B trajectories) are dominated by the mirror force, which doesn't modify the particle's energy, and do therefore roughly move along circles (Figure 2, dashed curves) although they still gain some energy in the electrostatic field. For a proton with a final velocity of $v_\perp = v_{\perp,\mathrm{crit}}$ the combined action of both the electrostatic and the mirror force causes the particle to move along a path of constant phase space density so that, as shown in Figure 2, the initial distribution function remains unchanged at that particular value of $v_\perp$.

Protons of type C are resonant (i.e., they do not circulate) and can be thought to be immobile as the wave grows. They mainly increase their $v_\perp$, owing to betatron acceleration in the steadily increasing magnetic field intensity. Although the strength of the electrostatic force on a particle is independent of its velocity (see (9)), the kinetic energy change of the particle, due to the electrostatic potential, isn't. In fact, from (2) it appears that for a resonant particle the energy change, due to the electric field, is significantly smaller than for a nonresonant particle. In particular, at $v_\parallel = 0$ the energy change, due to the electrostatic field, vanishes and the particle behaves exactly as described by *Southwood and Kivelson* [1993]; that is, only $v_\perp$ changes (Figure 2, path C). Equation (10) confirms that δf_p is unaffected at $v_\parallel = 0$, anticipating that although many aspects of the mirror instability which are connected with the circulating protons are modified by a nonzero T_e, the basic physics of the instability, which crucially depends on the resonant protons, is preserved even for large values of the electron temperature.

The dependence of $(v_{\perp,\mathrm{crit}}/v_{T\perp})^2$ on the electron temperature is illustrated by the dashed curve in Figure 3. It is interesting to note that in the case of a bi-Maxwellian proton distribution the same curve represents the ratio $-\delta N_{E\parallel}/\delta N_{\mathrm{mir}}$ of the density of protons being dominated by the $\delta E_\parallel$ field to the density of protons being dominated by the mirror force (obtained by integrating over velocity space the last and the first term, respectively, on the left-hand side of (10)). This ratio is always less than unity, so that the anticorrelation between δN_p and $\delta B_\parallel$ is preserved for all values of T_e at least as long as neglecting the contribution from the resonant protons to δN_p is justified (see section 2.4). This also follows from the perspective of the electrons

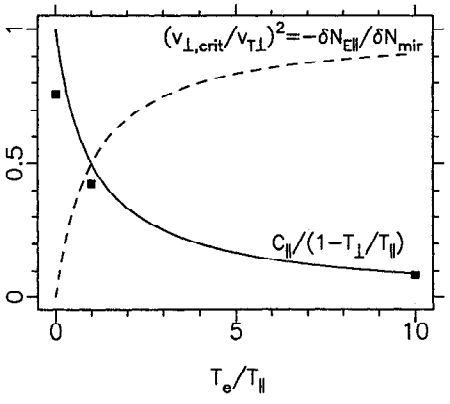

Figure 3. Normalized square critical velocity $v^2_{\perp,\mathrm{crit}}/v^2_{T\perp}$ (dashed curve) and parallel compressibility $C_\parallel$ (solid curve) as a function of $T_e/T_\parallel$ for the case $\beta_\parallel = 1$ and $T_\perp/T_\parallel = 1.8$ (equations (12) and (24)). The squares denote the normalized parallel compressibility for the fastest growing mode calculated by numerically solving the full Vlasov dispersion relation for three different values of $T_e/T_\parallel$ for the case $T_\perp/T_\parallel = 1.8$ and $\beta_\parallel = 1$ (see section 3 in text and Table 1).

being dragged by the protons, so that the sense of proton behavior can not be reversed by the longitudinal electric field.

Since the electron temperature is isotropic, the expression for δf_e in (11) contains only two terms which are the counterparts of the last two in the expression for δf_p. For all practical applications the contribution from the resonant electrons can be neglected, as can be understood from the following arguments. In the case of $T_e \neq 0$ the number of resonant electrons is less than that of the protons by a factor $\sim (T_\parallel m_e/T_e m_p)^{1/2}$ which is less than unity unless the electron temperature is $O(10^{-3}T_\parallel)$. Similarly, the relative energy densities of resonant warm electrons to protons is less than unity unless the electron temperature exceeds that of the protons by a factor $O(m_p/m_e) \sim 10^3$. We shall not consider the case of very cold electrons such that they all lie within the resonance. We note, however, that we are considering the $\gamma \to 0$ limit here, for which the resonance formally shrinks to zero. Thus we can recover previous results which ignored the electron pressure by taking the $T_e \to 0$ limit of our results without contradicting the fluidlike electron behavior which corresponds, in fact, to consideration of only the nonresonant electron population. Thus the perturbed electron distribution is essentially described by the last term on the right-hand side of (11) which simply compensates for the circulating protons which correspond to the first term on the right-hand side of (10). In this limit the light electrons are passively carried around by the massive protons and thus can be interpreted as a massless neutralizing fluid.

2.2. The Dispersion Relation

We now calculate the dispersion relation following *Southwood and Kivelson* [1993] by imposing a pressure balance condition which in the double-adiabatic (or CGL) theory [e.g., *Krall and Trivelpiece*, 1973, chapter 3.10] reads

$$\nabla_\perp \left(p_\perp + \frac{B^2}{8\pi}\right) - \frac{(\mathbf{B}\cdot\nabla)\mathbf{B}}{4\pi}\left(\frac{p_\perp - p_\parallel}{B^2/8\pi} + 1\right) = 0 \tag{13}$$

from which the x component yields (remembering that $k_\perp \delta B_x + k_\parallel \delta B_\parallel = 0$)

$$\delta p_{e\perp} + \delta p_\perp + \frac{B_0 \delta B_\parallel}{4\pi}\left[1 + \left(\frac{k_\parallel}{k_\perp}\right)^2 (\beta_\perp - \beta_\parallel + 1)\right] = 0 \tag{14}$$

with $\beta_\parallel = \beta_\perp T_\parallel/T_\perp$. By consistently omitting the contribution from the resonant electrons (electrons are therefore treated in the fluid approximation) and by finding the pressure perturbations in (14) by taking the second moments of (10) and (11), one obtains the fol-

lowing expression for the growth rate of the proton mirror instability

$$-\frac{\gamma}{k_{\parallel}v_{T\parallel}} = \frac{1+\left(\frac{k_{\parallel}}{k_{\perp}}\right)^2(\beta_{\perp}-\beta_{\parallel}+1)}{\beta_{\perp}\sqrt{\pi}\frac{T_{\perp}}{T_{\parallel}}\left[1-\frac{1}{2}\left(1-\frac{T_{\parallel}}{T_{\perp}}\right)\frac{T_e}{T_e+T_{\parallel}}\right]} - \frac{1}{\sqrt{\pi}}\left(1-\frac{T_{\parallel}}{T_{\perp}}\right) \quad (15)$$

where we have supposed that $|\gamma/k_{\parallel}v_{T\parallel}| \ll 1$, which is to say that the ratio of resonant to nonresonant protons is small, and where in the limit $T_e \to 0$ and $k_{\parallel}/k_{\perp} \ll 1$ the result of *Southwood and Kivelson* [1993] is recovered. The first term on the right-hand side of (15), which depends on T_e, is always positive and represents the damping element of the mode, while the second term provides the wave growth. It is obvious from (15) that the $k_{\perp} \gg k_{\parallel}$ limit yields a growing mode for the smallest temperature anisotropy. However, since $\gamma \propto k_{\parallel}$, this limit can only be obtained by letting $k_{\perp}$ tend to infinity. In practice, finite Larmor radius effects determine the $k_{\perp}$ at maximum growth rate. The nonzero electron temperature increases the damping term essentially because as T_e increases the contribution from nonresonant particles (electrons and protons) to the pressure perturbation in (14) decreases (since it is proportional to $(T_e+T_{\perp})/(T_e+T_{\parallel})$), so that the contribution from resonant protons, which, as discussed by Southwood and Kivelson, is essentially proportional to γ and of opposite sign, must be smaller to ensure pressure balance.

According to (15) and for a fixed k, maximum growth occurs at $(k_{\parallel}/k_{\perp})^2_{\max}$ given by

$$\left(\frac{k_{\parallel}}{k_{\perp}}\right)^2_{\max} = A\left[1+\frac{2}{3}\left(\frac{k_{\parallel}}{k_{\perp}}\right)^2_{\max}\right]^{-1} \quad (16)$$

with

$$A \equiv \frac{\left(\frac{T_{\perp}}{T_{\parallel}}-1\right)\left[1-\frac{1}{2}\left(1-\frac{T_{\parallel}}{T_{\perp}}\right)\frac{T_e}{T_e+T_{\parallel}}\right]-\beta_{\perp}^{-1}}{3\beta_{\perp}^{-1}(\beta_{\perp}-\beta_{\parallel}+1)}.$$

Near to the instability threshold, only modes satisfying $(k_{\parallel}/k_{\perp})^2_{\max} \ll 1$ are unstable. Thus

$$\left(\frac{k_{\parallel}}{k_{\perp}}\right)^2_{\max} \simeq A \quad (17)$$

provides a good estimate of the **k** vector orientation at maximum growth under weakly unstable conditions. Equation (16) (or (17)) shows that a nonzero electron temperature has the effect of making the wave vector of the fastest growing mode more perpendicular. From (15) it is also possible to obtain an estimate of the upper limit for the range of $(k_{\parallel}/k_{\perp})$ above which unstable modes can't exist (the lower limit being, of course, $k_{\parallel}/k_{\perp}=0$). This limiting value $(k_{\parallel}/k_{\perp})_0$ is determined by the vanishing of the right-hand side of (15) which occurs at

$$\left(\frac{k_{\parallel}}{k_{\perp}}\right)^2_0 = 3A \quad (18)$$

which is close to the value found by *Barnes* [1966]. In Figure 4 the functional dependence of θ_{kB} (which denotes the angle between the direction of the magnetic field $\mathbf{B}_0$ and the wave vector of the fastest growing mode) on the electron temperature is shown for the case $\beta_{\parallel}=1$ and different values of $T_{\perp}/T_{\parallel}$. As could be deduced immediately by inspection of (16) (or (17)), the dependence is rather strong for $T_e \lesssim T_{\parallel}$ especially as $T_{\perp}/T_{\parallel}$ approaches the stability threshold. From (16) (or (17)) it also appears that for $T_e/T_{\parallel} \gg 1$ the ratio $(k_{\parallel}/k_{\perp})_{\max}$ approaches a finite value for which, given a sufficiently high anisotropy $T_{\perp}/T_{\parallel}$, the mode may remain unstable. However, as stated earlier, for $T_e/T_{\parallel} \gtrsim O(m_p/m_e)$ the energy carried by the resonant electrons exceeds that of the resonant protons, and the approximations made in the present model are no longer valid.

A further remark is in order here about the fact that even though θ_{kB} is assumed to be close to 90° (which is the case just above the instability threshold), the theory turns out to work well even for fairly oblique wave vectors in which case, however, the term with $(k_{\parallel}/k_{\perp})^2$ in (15) is no longer negligible and the growth rate may substantially depend on it. Also from (15) it follows that maximum growth occurs for $k_{\perp}, k_{\parallel} \to \infty$. This is obviously wrong, and the reason is that the CGL pres-

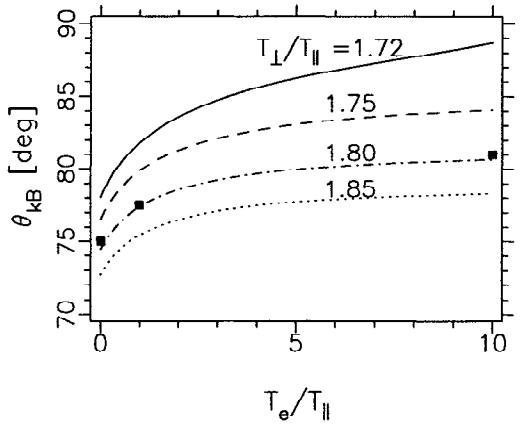

Figure 4. Curves showing the dependence of the angle θ_{kB} between the wave vector of the most unstable mode and the background magnetic field $\mathbf{B}_0$ as a function of $T_e/T_{\parallel}$ for different values of $T_{\perp}/T_{\parallel}$ in the case of $\beta_{\parallel}=1$ (equation (16)). As in Figure 3, squares denote values of θ_{kB} for the fastest growing mode found by numerically solving the full Vlasov dispersion relation for three different values of $T_e/T_{\parallel}$ in the case $T_{\perp}/T_{\parallel}=1.8$ and $\beta_{\parallel}=1$.

sure balance condition is only a good approximation as long as the Larmor radius of a protons is small compared to the perpendicular scale length of the wave and as long as in one gyroperiod a proton guiding center sees a nearly uniform field, namely,

$$\frac{v_{T\perp}}{\Omega_p} \ll \frac{1}{k_\perp} \tag{19a}$$

$$\frac{v_{T\parallel}}{\Omega_p} \ll \frac{1}{k_\parallel} \tag{19b}$$

with $\Omega_p \equiv eB/mc$ being the proton cyclotron frequency. Thus for $k_\perp$ ($k_\parallel$) larger than some value, which is of order $\Omega_p/v_{T\perp}$ ($\Omega_p/v_{T\parallel}$), finite Larmor radius effects become important, damping takes over, and the growth rate isn't well approximated by (15) any more.

The instability threshold for the proton mirror mode in the presence of hot electrons can be deduced from (15) and (16) and reads

$$\beta_\perp^{-1} + \left(1 - \frac{T_\perp}{T_\parallel}\right)\left[1 - \frac{1}{2}\left(1 - \frac{T_\parallel}{T_\perp}\right)\frac{T_e}{T_e + T_\parallel}\right] = 0 \tag{20}$$

a result which has been obtained, in less explicit forms, by *Barnes* [1966], *Tajiri* [1967], and *Belmont et al.* [1992]. Curves of the instability threshold for three different values of $\beta_\parallel$ are shown in Figure 5. The curves show that the sensitivity of the instability threshold on the electron temperature is rather weak unless $\beta_\parallel$ is small. Under such conditions, instability is only possible for high anisotropies $T_\perp/T_\parallel \gg 1$ in which case the last term in (20) eventually becomes important.

Although the instability threshold is only slightly modified by the hot electrons, this is not true for the growth rate. Figure 6 shows the growth rate of the fastest growing mode as a function of $T_e/T_\parallel$ for $\beta_\parallel = 1$ and three different values of $T_\perp/T_\parallel$. The growth rate is

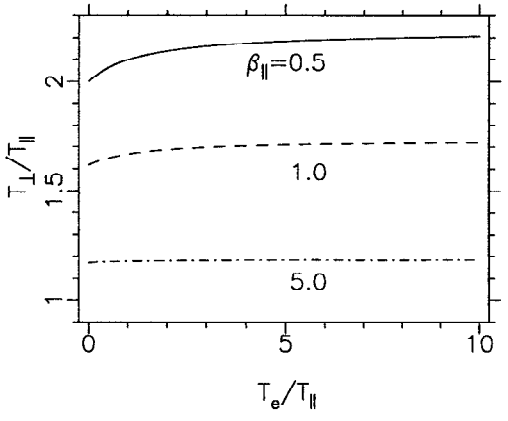

Figure 5. Instability threshold predicted by the model (equation (20)) as a function of $T_e/T_\parallel$ for three different values of $\beta_\parallel$. The unstable regions are located above the respective curves. Note the weakly stabilizing effect of an increasing T_e, particularly visible at low $\beta_\parallel$.

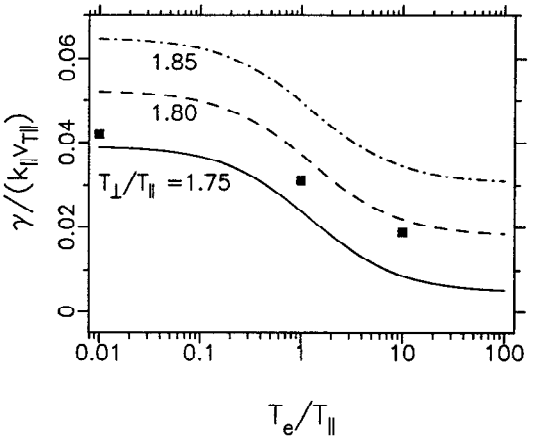

Figure 6. Growth rate of the most unstable mode for three different values of proton temperature anisotropy $T_\perp/T_\parallel$ (equation (15)). Unlike the instability threshold, which is only weakly dependent on T_e, the growth rate is seen to depend significantly on the electron temperature for $T_e/T_\parallel = O(1)$. Again, squares indicate the results for the fastest growing mode from the full Vlasov dispersion relation for the case $T_\perp/T_\parallel = 1.8$ and $\beta_\parallel = 1$.

naturally seen to increase with increasing $T_\perp/T_\parallel$, and the curves are found to depend strongly on T_e over a rather broad range around $T_e/T_\parallel = O(1)$. Note that at some value of $T_\perp/T_\parallel$ the curves eventually cross the $\gamma = 0$ axis, as the instability threshold, given by equation (20), depends on T_e.

The reason for the squares in Figure 6, indicating the results from the full Vlasov dispersion relation, being systematically below the $T_\perp/T_\parallel$ curve is mainly due to finite Larmor radius effects. The discrepancies between the theory and the numerical results vanish in the long-wavelength limit as the temperature anisotropy approaches the stability threshold given by (20).

2.3. Polarization

Concerning the mirror mode's polarization, we note that combining Faraday's equation $\gamma\delta B_\parallel = -ick_\perp\delta E_y$ (with $k_\perp$ pointing in the x direction, and c denoting the speed of light) and (9) we can explicitly evaluate $\delta\epsilon_\parallel$ defined as

$$\begin{aligned}\delta\epsilon_\parallel &\equiv \frac{\delta E_\parallel}{\delta E_y}\left(\frac{\Omega_p}{k_\perp v_{T\parallel}}\right) \\ &= \frac{k_\parallel v_{T\parallel}}{2\gamma}\left(\frac{T_\perp - T_\parallel}{T_e + T_\parallel}\right)\frac{T_e}{T_\parallel}\end{aligned} \tag{21}$$

where γ is given by (15). The quantity $\delta\epsilon_\parallel$ has the advantage over the usual ratio $\delta E_\parallel/\delta E_y$ that it is independent of $k_\perp$ (which can't be computed from the model). The dependence of the effective polarization $\delta E_\parallel/\delta E_y$ on T_e is obviously not the same as the dependence of $\delta\epsilon_\parallel$ on T_e since $k_\perp$ itself is generally a function of T_e. However, as we will show below, the T_e depen-

dence of the polarization is extremely strong, while it is heuristically clear that $k_\perp$ of the fastest growing mode is roughly determined by the appearance of finite proton Larmor radius effects so that $k_\perp \sim \Omega_p/v_{T\perp}$ independent of the electron temperature. In an example which will be discussed in section 3 we show, by solving numerically the full Vlasov dispersion relation (see Table 1), that increasing the electron temperature by a factor of 1000 (from $T_e/T_\parallel = 0.01$ to 10) only reduces by 66% the value of $k_\perp$ for the fastest growing mode. On the other hand, (21) applied to the same example shows that, taken over the same temperature range, $\delta c_\parallel$ rises by 2 orders of magnitude (see the lower solid line in Figure 7).

As pointed out by *Hasegawa* [1969] in the cold electron limit, only the y component of the electric field fluctuation is finite. In fact, (9) reveals that in the limit $T_e \to 0$ one has that $\delta E_\parallel \to 0$, and since no charge separation can occur in this limit, Poisson's equation reduces to $k_\perp \delta E_x + k_\parallel \delta E_\parallel = 0$ which also implies $\delta E_x = 0$. On the other hand, the mirror mode must satisfy $\delta B_y = 0$ in order to prevent the mode from acquiring characteristics associated with the transverse Alfvén mode (the y component of the magnetic field fluctuation never appears in the model since for a given $\delta B_\parallel$, only δB_x is fixed by the condition $\nabla \cdot \delta\mathbf{B} = 0$). Thus we have $(\nabla \times \delta\mathbf{E})_y = 0$, i.e.,

$$\frac{\delta E_x}{\delta E_\parallel} = \frac{k_\perp}{k_\parallel} \tag{22}$$

which at maximum growth can be computed from (16). Finally, combining (21) and (22), we obtain

$$\delta\epsilon_x \equiv \frac{\delta E_x}{\delta E_y}\left(\frac{\Omega_p}{k_\perp v_{T\parallel}}\right) = \frac{k_\perp}{k_\parallel}\delta\epsilon_\parallel. \tag{23}$$

From (21) and (23) we deduce that both $\delta\epsilon_x$ and $\delta\epsilon_\parallel$ increase with T_e. Thus the effect of increasing the electron temperature is to switch the electric field from the y direction into the plane perpendicular to it. The quantities $\delta\epsilon_\parallel$ and $\delta\epsilon_x$ are reproduced in Figure 7 for the fastest growing mode, in the case $\beta_\parallel = 1$ and $T_\perp/T_\parallel = 1.8$ (solid curves) and $T_\perp/T_\parallel = 1.85$ (dashed curves). The dependence of the polarization on the electron temperature is very strong for $T_e/T_\parallel \lesssim 1$, while both $\delta\epsilon_\parallel$ and $\delta\epsilon_x$ saturate at some value as $T_e \gg T_\parallel$ (note that one has always $\delta\epsilon_x/\delta\epsilon_\parallel = k_\perp/k_\parallel$). The differences between the solid and dashed curves indicate that as $T_\perp/T_\parallel$ is increased, the mirror component of the electric field δE_y is also increased relative to the components in the $(\mathbf{k}, \mathbf{B}_0)$ plane. Figure 7 also shows that polarization measurements in linear mirror waves are an extremely sensitive measure of the electron temperature.

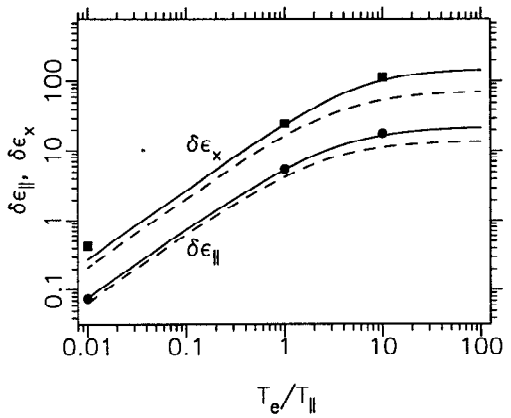

Figure 7. Normalized polarizations $\delta\epsilon_\parallel$ and $\delta\epsilon_x$ for the case $\beta_\parallel = 1$ and $T_\perp/T_\parallel = 1.8$ and 1.85 (solid and dashed curves, respectively). Squares (denoting $\delta\epsilon_x$) and circles (denoting $\delta\epsilon_\parallel$) correspond to the fastest growing mode determined from the full Vlasov dispersion relation in the case $T_\perp/T_\parallel = 1.8$ and $\beta_\parallel = 1$.

2.4. The Parallel Compressibility

In the case of a nonzero T_e the accumulation of electrons in regions of low parallel magnetic field density increases the electron pressure there. As expressed by (8) the electron pressure gradient between low and high parallel magnetic field has to be compensated by a longitudinal electric field. How strongly T_e, through $\delta E_\parallel$, acts against the development of the characteristic magnetic field-density anticorrelation can be quantified by computing the parallel compressibility $C_\parallel$ [cf. *Lacombe*

Table 1. Full Vlasov Dispersion Relation

Case	β_e	γ/Ω_p	$kv_{T\perp}/\Omega_p$	$\gamma/(k_\parallel v_{T\parallel})$	θ_{kB}	$Re(C_\parallel)$	$\delta\epsilon_\parallel$	$\delta\epsilon_x$
A	0.01	2.99×10^{-3}	0.369	4.20×10^{-2}	75°	−0.607	0.075	0.429
B	1	1.57×10^{-3}	0.313	3.11×10^{-2}	77.5°	−0.340	5.49	25.0
C	10	5.34×10^{-4}	0.243	1.88×10^{-2}	81°	−0.067	17.8	112.4

Properties of the most unstable modes for three different values of the ratio of the electron pressure to the magnetic field pressure β_e. Listed quantities are γ/Ω_p, the growth rate normalized to the proton cyclotron frequency; $kv_{T\perp}/\Omega_p$, the length of the wave vector normalized to the Larmor radius of a thermal proton; $\gamma/(k_\parallel v_{T\parallel})$, the width of the resonance normalized to the parallel proton thermal velocity; θ_{kB}, the angle between the wave vector and the magnetic field; $Re(C_\parallel)$, the real component of the parallel compressibility. Both $\delta\epsilon_\parallel$ and $\delta\epsilon_x$ are a measure of the the electric polarization of the mode (see section 2.3). The complete dispersion relation has been solved using WHAMP [*Rönnmark*, 1983]. Other plasma parameters are $T_\perp/T_\parallel = 1.8$, $\beta_\parallel = 1$ and $\omega_p/\Omega_p = 3.3 \times 10^3$.

Table 2. Model of Section 2

Case	β_e	$\gamma/(k_\parallel v_{T\parallel})$	θ_{kB}	$Re(C_\parallel)$	$\delta\epsilon_\parallel$	$\delta\epsilon_x$	$v_{\perp,\mathrm{crit}}/v_{T\perp}$
A	0.01	5.21×10^{-2}	74.1°	−0.80	0.078	0.275	0.099
B	1	3.72×10^{-2}	77.2°	−0.40	6.15	27.0	0.707
C	10	2.19×10^{-2}	80.6°	−0.073	21.0	126.4	0.953

Properties of the most unstable modes for the same cases as in Table 1. Listed quantities have same meaning as in Table 1 with $v_{\perp,\mathrm{crit}}/v_{T\perp}$ denoting the temperature-dependent critical velocity given by equation (12). All quantities have been calculated using the model presented in section 2. Note the good agreement with the corresponding quantities listed in Table 1.

et al., 1992] explicitly. $C_\parallel$ has a vanishing imaginary part because δN_p and δN_e are out of phase by 180° with respect to $\delta B_\parallel$ and is easily found from (8) and (9) to be given by

$$C_\parallel = \frac{\delta N_p}{N_0}\frac{B_0}{\delta B_\parallel} = \frac{\delta N_e}{N_0}\frac{B_0}{\delta B_\parallel} = \frac{T_\parallel - T_\perp}{T_e + T_\parallel} < 0 \qquad (24)$$

which goes to 0 as $T_e \to \infty$ and to the cold electron limit as $T_e \to 0$. Also note that the cold electron limit obtained by *Hasegawa* [1969] is identical to the result found by *Belmont et al.* [1992] since near to the instability threshold, one has $C_\parallel = \beta_\perp^{-1} = (1 - T_\perp/T_\parallel)$. From (24) it appears that whenever T_e is of the same order or larger than $T_\parallel$, the compressibility strongly differs from the cold electron limit as illustrated by the solid curve in Figure 3. This has to do with the fact that as $v_{\perp,\mathrm{crit}}$ becomes of the same order of $v_{T\perp}$, a significant fraction of circulating (i.e., nonresonant) protons are being dominated by the longitudinal electric field rather than by the mirror force. The fact that even for very hot electrons, one always has $v_{\perp,\mathrm{crit}} < v_{T\perp}$ ensures that the mirror force always overcomes the electrostatic force for protons with $v_\perp \geq v_{T\perp}$ and thus $C_\parallel < 0$ even for $T_e \gg T_\parallel$. Other transport ratios can obviously be calculated using (10) and (11).

It has to be pointed out at this stage that most of the conclusions in the above model and, in particular, the ones for $C_\parallel$, are based on the critical assumption that the contributions of the resonant protons to the moments is negligible except for determining the growth rate (i.e., (15)). Taking the zeroth order moment of (10), we find that the contribution to the density perturbation δN_p from the resonant protons is small provided the following inequality holds

$$\frac{|\gamma|}{k_\parallel v_{T\parallel}} \ll \frac{1}{\sqrt{\pi}}\frac{T_\perp - T_\parallel}{T_e + T_\perp}. \qquad (25)$$

This is a necessary condition for the above estimates of $C_\parallel$ to be valid. If (25) is violated, the contribution of the resonant protons to δN_p has then to be retained in the theory in order to get the correct expressions.

3. Testing the Model

In order to test the validity of the model presented in section 2, we compare its results with the results from the full Vlasov dispersion relation. We use the program WHAMP (Waves in Homogeneous Anisotropic Multicomponent Plasmas) [*Rönnmark*, 1983] to solve the dispersion relation for three different electron temperatures such that $\beta_e = 0.01, 1, 10$ (cases A, B, and C) with all other plasma parameters being the same for the three cases. These are $T_\perp/T_\parallel = 1.8$, $\beta_\parallel = 1$, and the ratio of the proton plasma frequency to the proton cyclotron frequency $\omega_p/\Omega_p = 3.3 \times 10^3$ which is of the order of solar wind values. Note that the actual value of ω_p/Ω_p is irrelevant here as long as it is $\gg 1$ which is an implicit assumption of the above nonrelativistic model. The characteristics of the most unstable modes in the three cases are given in Table 1. As required by the model, the growth rates are small compared to the proton cyclotron frequency Ω_p and $(k_\parallel/k_\perp)^2 \ll 1$. It appears from Table 1 that the wavelength of the most unstable mode only increases by a factor of about 1.5 between case A and C, while the absolute value of the parallel compressibility drops by as much as 1 order of magnitude. The values of $C_\parallel$ from Table 1 are also reported in Figure 3 (solid squares) showing a good agreement with the curve from the model.

In Table 2 the results of the model applied to the three above cases are shown. For all listed quantities the agreement between the results from the full Vlasov dispersion relation and the model is quite satisfactory. Even the wave vector angle θ_{kB} and the polarization computed in section 2 (see figures 4 and 7) agree well with the corresponding quantities from WHAMP listed in Table 1 suggesting that the model takes into account most of the relevant features of the instability in a nonzero electron temperature plasma. The reason why the model systematically overestimates the growth rates from WHAMP stems from the fact that finite Larmor radius effects, which have a damping effect on the mirror mode, have not been retained in our calculations. Finite Larmor radius effects are, of course, the reason for the growth rate $\gamma(k)$ computed from WHAMP, to peak at values of k which are of the order of $\Omega_p/v_{T\perp}$ (see Table 1).

Figure 8 shows the distribution function $\delta f(v_\parallel, v_\perp)$ for cases A, B, and C at a position corresponding to a maximum of the parallel magnetic field flux $|B_0 + \delta B_\parallel|$. The δf_p has been obtained by numerically following proton phase space trajectories through the field of the

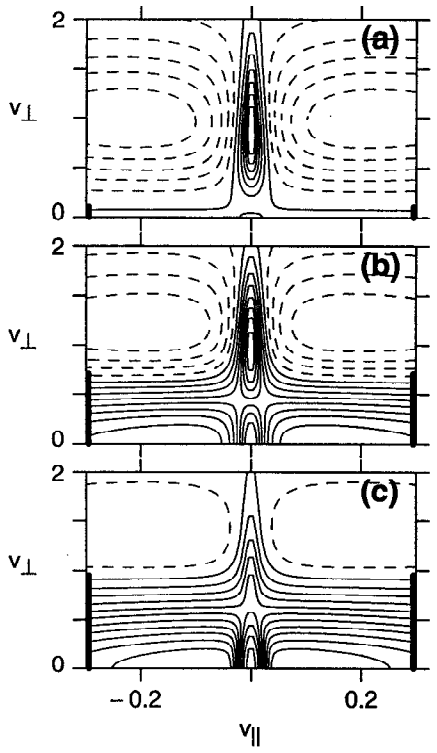

Figure 8. The perturbation of the distribution function $\delta f_p(v_\parallel, v_\perp)$ calculated from complete linear theory at a maximum of $|B_0 + \delta B_\parallel|$ for the (a) case A, (b) case B, and (c) case C in Table 1. Solid (dashed) lines denote positive (negative) equidistant contours. The black stripes denote $v_\perp < v_{\perp,\mathrm{crit}}$, where $v_{\perp,crit}$ is given by equation (12). This figure should be compared with the schematic picture in Figure 2.

growing linear waves given in Table 2 and by applying the Liouville theorem starting from the unperturbed distribution function $f_p(v_\parallel, v_\perp)$ (details of the method are given by *Pantellini et al.* [1994]). The results of Figure 8, of course, depend on the final amplitude of the wave. However, as long as $\delta B_\parallel/B_0 \ll 1$ (in figure 8 the final amplitudes are $\lesssim 0.01$), δf scales with $\delta B_\parallel/B_0$ apart from negligible small corrections proportional to $(\delta B_\parallel/B_0)^2$. Since the wave field seen by a proton varies slowly in space and time (see above), the drift equations [cf. *Morozov and Solov'ev*, 1966)] have been used in place of the full equations of motion.

The thick solid bars in Figure 8 indicate the region $v_\perp < v_{\perp,\mathrm{crit}}$ as given by (12) (compare Table 2). From Figure 8 it appears that $v_{\perp,\mathrm{crit}}$ gives an excellent estimate of the position of sign reversal in f_p, suggesting that δf_p as given by (10) is a good approximation to the linear perturbation of the proton distribution function. Note that for Figure 8a the region $v_\perp < v_{\perp,\mathrm{crit}}$ is negligibly small; in this case the cold electron model applies and only the circulating (dashed contours) as well as the resonant protons (solid contours centered around $|v_\parallel| \lesssim |\gamma/k_\parallel| \ll v_{T\parallel}$), are important. Figure 8b shows that as T_e becomes of the same order of $T_\parallel$, a non-negligible number of protons with small perpendicular velocity ($\lesssim v_{\perp,\mathrm{crit}}$) become dominated by the longitudinal electric field. For $T_e \gg T_\parallel$ (Figure 8c), protons dominated by longitudinal electric field cover nearly the whole region with $v_\perp < v_{T\perp}$. In this case the proton distribution function bears little resemblance to the cold electron limit distribution of panel Figure 8a. Owing to the fact that the compressibilities calculated from the model and from the full Vlasov dispersion relation are in excellent agreement (compare Figure 3 and both Tables 1 and 2), it is not surprising that values for $v_{\perp,\mathrm{crit}}$, estimated from (12), are a good estimate of the position of sign reversal of δf_p as shown in Figure 8 for all three cases. A final comment on Figure 8 is that as the spatial dependence of the linear response δf_p is given by $\exp[i(k_\perp x + k_\parallel z)]$, one has that at a minimum of the parallel magnetic field flux, δf_p is just the negative of δf_p at a maximum of the parallel magnetic field flux.

It should also be emphasized that the discrepancies between the numerical solutions and the model tend to shrink as one approaches the stability threshold given by (20) and if one takes the long-wavelength limit $k \to 0$. However, here we show that the model gives good estimates of the characteristics, including the T_e dependencies, of the most unstable mode even in the case of fairly oblique (i.e., relatively fast growing) instabilities. From this detailed comparison of the analytical results derived in section 2 with the results from WHAMP we conclude that the model presented in section 2 gives a good description of the slowly growing proton mirror instability in a proton-electron plasma with $T_e \neq 0$.

4. Conclusion

We have presented a model for the long-wavelength proton mirror instability when a nonzero temperature electron population is included. The model shows that as expected, the nonzero temperature of the electrons decreases the growth rate and modifies the instability threshold, as well as θ_{kB}, of the fastest growing mode. Apart from causing a significant reduction in the values of the parallel compressibility $C_\parallel$, the hot electrons strongly modify the mode's polarization causing the electric field fluctuations to turn into the $(\mathbf{k}, \mathbf{B}_0)$ plane. All these effects are ultimately due to a longitudinal field which arises because an electron pressure gradient builds up as the electrons are dragged by the circulating protons from the high into the low parallel magnetic field flux regions. The longitudinal electric field, which for positively charged particles acts against the mirror force, prevents protons with $v_\perp < v_{\perp,\mathrm{crit}}$ from responding in the usual way to the magnetic field perturbations.

The effects of the nonzero electron temperature are seen to be important whenever $T_e/T_\parallel = O(1)$. This is a value which is easily encountered in the solar wind and even in magnetospheric plasmas where, as a result, the cold electron model by *Southwood and Kivelson* [1993]

may not be applicable. The effect of a nonzero electron temperature on the proton distribution function at a maximum of the parallel magnetic field flux is shown in Figures 2 and 8. Figure 2 and Figures 8b and 8c differ from *Southwood and Kivelson* [1993, Figure 2] in that the density of protons with $v_\perp < v_{\perp,\mathrm{crit}}$ is increasing and not decreasing as the instability develops. The fact that these protons are not mirror accelerated as are the ones with $v_\perp \geq v_{\perp,\mathrm{crit}}$, added to the fact that their number is a sensitive function of $T_e/T_\parallel$, is the reason most of the characteristics of the proton mirror mode are strongly dependent on the electron temperature.

Acknowledgments. This work has been supported by SERC (UK) grant GR/H09454 and the Commission of the European Community under contract SCI0468-M. The authors express their thanks to K. Rönnmark for kindly supplying the WHAMP program.

The Editor thanks M. Kivelson and S.P. Gary for their assistance in evaluating this paper.

References

Anderson, B.J., and S.A. Fuselier, Magnetic pulsations from 0.1 to 0.4 Hz and associated plasma properties in the Earth's subsolar magnetosheath and plasma depletion layer, *J. Geophys. Res.*, *98*, 1461, 1993.

Anderson, B.J., S.A. Fuselier, S.P. Gary, and R.E. Denton, Magnetic spectral signatures in the Earth's magnetosheath and plasma depletion layer, *J. Geophys. Res.*, *99*, 5877, 1994.

Barnes, A., Collisionless damping of hydromagnetic waves, *Phys. Fluids, 9*, 1483, 1966.

Belmont, G., D. Hubert, C. Lacombe, and F. Pantellini, Mirror mode and other compressive ULF modes, in Proceedings of the 26th ESLAB Symposium on the Study of the Solar-Terrestrial System, *Eur. Space Agency Spec. Publ. ESA SP-346*, 263, 1992.

Chandrasekhar, S., A.N. Kaufman, and K.M. Watson, The stability of the pinch, *Proc. R. Soc. London, A, 245*, 435, 1958.

Davidson, R.C., and J.M. Ogden, Electromagnetic ion cyclotron instability driven by ion energy anisotropy in high–beta plasmas, *Phys. Fluids, 18*, 1045, 1975.

Gary, S.P., The mirror and ion cyclotron anisotropy instabilities, *J. Geophys. Res.*, *97*, 8519, 1992.

Hasegawa A., Drift mirror instability in the magnetosphere, *Phys. Fluids, 12*, 2642, 1969.

Hubert, D., C. Perche, C.C. Harvey, C. Lacombe, and C.T. Russell, Observation of mirror waves downstream of a quasi–perpendicular shock, *Geophys. Res. Lett.*, *16*, 159, 1989.

Jeffrey, A., and T. Taniuti, *Magnetohydrodynamic Stability and Thermonuclear Containment*, Academic, San Diego, Calif., 1966.

Kaufmann, R.L, J.T. Horng, and A. Wolfe, Large amplitude hydromagnetic waves in the inner magnetosheath, *J. Geophys. Res.*, *75*, 4666, 1970.

Krall, N.A., and A.W. Trivelpiece, *Principles of Plasma Physics*, McGraw-Hill, New York, 1973.

Lacombe, C., F.G.E. Pantellini, D. Hubert, C.C. Harvey, A. Mangeney, G. Belmont, and C.T. Russell, Mirror and Alfvénic waves observed by ISEE1–2 during crossing of the Earth's bow shock, *Ann. Geophysicae, 10*, 772, 1992.

McKean, M.E., D. Winske, and S.P. Gary, Mirror and ion cyclotron anisotropy instabilities in the magnetosheath, *J. Geophys. Res.*, *97*, 19,421, 1992.

McKean, M.E., S.P. Gary, and D. Winske, Kinetic physics of the mirror instability, *J. Geophys. Res.*, *98*, 21,313, 1993.

Morozov, A.I, and L.S. Solov'ev, Motion of charged particles in electromagnetic fields, in *Reviews of Plasma Physics, vol. 2*, Consultants Bureau, New York, 1966.

Northrop, T.G., *The Adiabatic Motion of Charged Particles*, p. 12, Wiley Interscience, New York, 1963.

Pantellini, F.G.E., D. Burgess, and S.J. Schwartz, Phase space evolution in linear instabilities, *Phys. Plasmas, 1*, 3784, 1994.

Pantellini, F.G.E., D. Burgess, and S.J. Schwartz, On the non linear mirror instability, *Adv. Space Res.*, in press, 1995.

Price, C.P., D.W. Swift, and L.C. Lee, Numerical simulation of nonoscillatory mirror waves at the Earth's magnetosheath, *J. Geophys. Res.*, *91*, 101, 1986.

Rönnmark, K., Computation of the dielectric tensor of a Maxwellian plasma, *Plasma Phys. Controlled Fusion, 25*, 699, 1983.

Rose, D.J., General criterion for mirror instability of a plasma, *Phys. Fluids, 8*, 951, 1965.

Russell, C.T., W. Riedler, K. Schwingenshuh, and Ye. Yeroshenko, Mirror instability in the magnetosphere of Comet Halley, *Geophys. Res. Lett.*, *14*, 664, 1987.

Southwood, D.J., and M.G. Kivelson, Mirror instability, 1, The physical mechanism of linear instability, *J. Geophys. Res.*, *98*, 9181, 1993.

Tajiri, M., Propagation of hydromagnetic waves in collisionless plasma, 2, Kinetic approach, *J. Phys. Soc. Jpn.*, *22*, 1482, 1967.

Tsurutani, B.T., D.J. Southwood, E.J. Smith, and A. Balogh, Nonlincar magnetosonic waves and mirror mode structures in the March 1991 Ulysses interplanetary event, *Geophys. Res. Lett.*, *19*, 1267, 1992.

Winske, D., and K.B. Quest, Magnetic field and density fluctuations at perpendicular supercritical collisionless shocks, *J. Geophys. Res.*, *93*, 9681, 1988.

F.G.E. Pantellini, Observatoire de Paris, Département de Recherche Spatiale, 92195 Meudon Cédex, France. (e-mail: pantellini@megasx.obspm.fr)

S.J. Schwartz, Astronomy Unit, Queen Mary and Westfield College, Mile End Road, London E1 4NS, England, United Kingdom. (e-mail: S.J.Schwartz@qmw.ac.uk)

(Received June 17, 1994; revised September 23, 1994; accepted September 23, 1994.)